

IUPAC Task Group on Atmospheric Chemical Kinetic Data Evaluation – Data Sheet P7

Datasheets can be downloaded for personal use only and must not be retransmitted or disseminated either electronically or in hardcopy without explicit written permission.

The citation for this data sheet is: IUPAC Task Group on Atmospheric Chemical Kinetic Data Evaluation, (<http://iupac.pole-ether.fr>).

This datasheet last evaluated: May 2013; last change in preferred values: May 2013.

CH₃COCH₃ + hv → products

Primary photochemical transitions

Reaction		$\Delta H^{\circ}_{298}/\text{kJ}\cdot\text{mol}^{-1}$	$\lambda_{\text{threshold}}/\text{nm}$
CH ₃ COCH ₃ + hv → CH ₃ CO + CH ₃	(1)	353.6	338
→ 2CH ₃ + CO	(2)	399.5	299

Absorption cross-section data

Wavelength range/nm	Reference	Comments
202-355	Martinez et al., 1992	(a)
260-360	Hynes et al., 1992	(b)
215-350	Gierczak et al., 1998	(c)
240-350	Yujing and Mellouki, 2000	(d)

Quantum yield data ($\phi = \phi_1 + \phi_2$)

Measurement	Wavelength range/nm	Reference	Comments
$\phi_1 = 0.76 - 0.0033$	250 - 330	Meyrahn et al., 1986	(e)
$\phi = 1.0 - 0.016$	248 - 337	Gierczak et al., 1998	(f)
$\phi_1 = 1.0 - 0.062$	280 - 330	Emrich and Warneck, 2000	(g)
$\phi = 1.0, 0.28$	248, 308	Aloisio and Francisco, 2000	(h)
$\phi_1 = 1.0 - 0.01$	279 – 327.5	Blitz et al., 2004	(i)
$\phi(\text{CO}) = 0.45$ (20 mbar) = 0.25 (900 mbar)	248	Somnitz et al., 2005	(j)
$\phi^0(\text{CO}) = 0.62$	250	Blitz et al., 2006	(k)
= 0.37	265		
= 0.13	285		
= 0.04	300		
= 0.012	313		
= 0.007	320		
$\phi = 0.581 \pm 0.062$ (13 mbar) = 0.527 ± 0.044 (33mbar) = 0.319 ± 0.032 (133 mbar) = 0.275 ± 0.010 (200 mbar) = 0.213 ± 0.016 (266 mbar) = 0.193 ± 0.034 (399 mbar) = 0.149 ± 0.024 (532 mbar) = 0.151 ± 0.010 (665 mbar)	308	Nadasdi et al., 2007	(l)

= 0.136 ± 0.022 (798 mbar)			
= 0.112 ± 0.008 (998 mbar)			
(298K)			
φ = 0.368 ± 0.002 (323K)	308		
= 0.319 ± 0.032 (298K)			
= 0.228 ± 0.002 (273K)			
= 0.178 ± 0.010 (253K)			
= 0.122 ± 0.014 (233K)			
(133 mbar)			
φ(CH ₃) = 1.42 ± 0.15 (7 mbar)	248	Khamaganov <i>et al.</i> , 2007	(m)
= 1.0 (2008 mbar)			
φ(CH ₃) = 0.92 ± 0.1	266		
φ ⁰ (CH ₃ CO) = 0.535 ± 0.09	248	Rajakumar, et al., 2008	(n)
= 0.82 (891 mbar)			
(296K)			
(298 K)	248	Khamaganov <i>et al.</i> , 2009	(o)
φ = 0.96 ± 0.05 (60 Torr)			
= 0.99 ± 0.04 (75 Torr)			
= 0.97 ± 0.06 (100 Torr)			
= 1.03 ± 0.08 (200 Torr)			
= 1.02 ± 0.10 (400 Torr)			
= 0.98 ± 0.04 (600 Torr)			
= 0.90 ± 0.10 (650 Torr)			
(224 K)			
φ = 1.04 ± 0.10 (75 Torr)			
(234 K)			
φ = 1.04 ± 0.15 (75 Torr)			
= 0.98 ± 0.05 (650 Torr)			
(298 K)	266		
φ = 0.93 ± 0.02 (60 Torr)			
= 1.00 ± 0.06 (100 Torr)			
= 0.97 ± 0.03 (200 Torr)			
= 0.88 ± 0.14 (300 Torr)			
= 0.81 ± 0.12 (400 Torr)			
= 0.88 ± 0.13 (500 Torr)			
= 0.90 ± 0.12 (593 Torr)			
= 0.82 ± 0.04 (700 Torr)			
= 0.84 ± 0.09 (760 Torr)			
(298 K)	300	Khamaganov and Crowley, 2013	(p)
φ = 0.74 ± 0.05 (60 Torr)			
= 0.66 ± 0.04 (100 Torr)			
= 0.54 ± 0.06 (200 Torr)			
= 0.43 ± 0.04 (300 Torr)			
= 0.31 ± 0.10 (500 Torr)			
= 0.27 ± 0.04 (740 Torr)			
(228 K)	300		
φ = 0.63 ± 0.04 (60 Torr)			
= 0.49 ± 0.04 (100 Torr)			
= 0.34 ± 0.03 (200 Torr)			
= 0.28 ± 0.04 (300 Torr)	308		
(298 K)			
φ = 0.50 ± 0.04 (30 Torr)			
= 0.35 ± 0.03 (60 Torr)			
= 0.29 ± 0.02 (100 Torr)			
= 0.23 ± 0.02 (200 Torr)			
(228 K)	308		

Comments

- (a) Cross-sections are the average values over a 1 nm ($\lambda > 280$ nm) or 4 nm ($\lambda < 280$ nm) region centered at the corresponding wavelength. $\sigma_{\max} = 5.07 \times 10^{-20}$ cm²molecule⁻¹ at 278 nm.
- (b) Cross-sections measured as a function of temperature over the range 260 K to 360 K. Data were presented in graphical form and show a marked decrease in cross-section with decreasing temperature at longer wavelengths.
- (c) Measurements made using a diode array spectrometer with a D₂ lamp source and temperature controlled cell with 200 cm path-length. Resolution 0.5 nm. Temperature range 235 – 298 K. Modest temperature dependence at $\lambda > 300$ nm. Tabulated cross sections at 1 nm intervals and parameterisation of temperature dependence given. $\sigma_{\max} = 4.94 \times 10^{-20}$ cm²molecule⁻¹ ($\pm 5\%$) at 278 nm.
- (d) Commercial diode array spectrometer with a D₂ lamp source and 200 cm pathlength cell at 298 K. Resolution 0.04 nm. Tabulated cross sections at 1 nm intervals given. $\sigma_{\max} = 4.97 \times 10^{-20}$ cm²molecule⁻¹ ($\pm 5\%$) at 278 nm.
- (e) Study of the quantum yield of formation of CO₂ and CO in the photolysis of dilute mixtures of acetone (0.13 mbar to 0.20 mbar) in air (990 mbar) at room temperature. In addition, the quantum yields of formation of peroxyacetyl nitrate (PAN) were measured when trace amounts of NO₂ (1.2×10^{-4} mbar) were added to the reactant mixtures. The listed values of ϕ_1 are the quantum yields of PAN, which were taken as a measure of the extent of primary process (1).
- (f) Quantum yield determined using pulsed laser photolysis of static mixtures with measurement of the loss of acetone and formation of product CO₂. ϕ was determined as a function of pressure (30-1000 mbar Air) and at nine discrete wavelengths in the stated range. At $\lambda > 270$ nm ϕ showed Stern-Volmer pressure quenching. The zero pressure quantum yield increased as wavelength decreased to a value of unity near 290 nm. At 308 nm ϕ was independent of temperature between 298 and 195 K. Expression given for the variation with pressure and wavelength of ϕ in air.
- (g) Quantum yields for peroxyacetyl nitrate (PAN) production from photodissociation of acetone ($< 1\%$) in air when trace amounts of NO₂ were added to the reactant mixtures. The quantum yields of PAN formation used to determine ϕ_1 at 10 nm intervals in the range given and at total pressures in the range 130-1000 mbar. Stern-Volmer pressure quenching observed at all wavelengths. Results interpreted in terms of the elementary processes involving the first excited singlet and triplet states of acetone, providing rate parameters for the competing processes as a function of excitation energy.
- (h) Relative quantum yield for acetone photodissociation at the specified laser wavelengths with and without water present. At a total pressure of 133 mbar, H₂O up to 12 mbar suppressed the quantum yield, the effect being stronger at 308 nm.
- (i) ϕ (CH₃CO) determined as a function of temperature (218-295 K) and pressure (0.46-540 mbar, [He, N₂ or Air]) using time-resolved HO-photofragment spectroscopy to monitor acetyl radical production from PLP of acetone (0.006 mbar). HO produced from CH₃CO + O₂ was monitored by LIF at 282 nm giving sensitivity of $< 10^8$ molecule cm⁻³. The total quantum yield $\phi_{\text{total}}(\lambda, p, T) = \phi_{\text{CH}_3\text{CO}}(\lambda, p, T) + \phi_{\text{CO}}(\lambda, T) = \phi_1 + \phi_2$ was determined relative to the measured values of $\phi_{\text{total}} = 1$, $\phi_{\text{CH}_3\text{CO}} = 0.65$ and $\phi_{\text{CO}} = 0.35$, at 248 nm and 295 K, at the zero pressure limit $p = 0$. Pressure dependence was represented by simple Stern-Volmer quenching at $\lambda < 302$ nm, but at longer wavelengths an extended form of Stern-Volmer expression was necessary to represent the data. A substantial decline in ϕ_{total} with decreasing temperature was observed at wavelengths above 310 nm. An empirical algorithm is given for the overall dissociation quantum yield, and for $\phi_{\text{CH}_3\text{CO}}$ and ϕ_{CO} in air, as a function of wavelength, temperature and pressure.

- (j) $\phi(\text{CO})$ determined as a function of pressure (20-900 mbar, $[\text{N}_2]$) at 298 K, using infrared diode laser absorption to monitor CO production from PLP of acetone at 248 nm. Results are interpreted to show CO production results exclusively from channel (1) via CH_3CO decomposition.
- (k) Measurements of $\phi(\text{CH}_3\text{CO})$ from acetone photolysis were made using PLP/LIF. $\phi_{\text{total}}(\lambda, p, T)$ was determined over the ranges: $266 < \lambda/\text{nm} < 327.5$, $0.3 < p/\text{Torr} < 400$ and $218 < T/\text{K} < 295$. $\phi(\text{CH}_3\text{CO})$ was determined relative to that at 248 nm by conversion to OH by reaction with O_2 . The cited values of $\phi(\text{CO})_\lambda$ are calculated from $(1 - \phi(\text{CH}_3\text{CO})_\lambda)_{M=0}$ obtained by Stern-Volmer analysis. Plots of $(1/[\text{OH}])$ vs $[\text{M}]$ were linear for $\lambda < 300$ nm, but for $\lambda > 300$ nm, nonlinear Stern-Volmer plots were observed. This behaviour is interpreted as evidence for dissociation from two excited states of acetone: S_1 when the Stern-Volmer plots are linear and both S_1 & T_1 when Stern-Volmer plots are nonlinear. A model for acetone photolysis is proposed that adequately describes both the present and literature data. Barriers to dissociation are invoked in order to explain the dependence of pressure quenching of the acetone photolysis yields as a function of wavelength and temperature. This pressure quenching was observed to become more efficient with increasing wavelength, but it was only at $\lambda \geq 300$ nm that a significant T dependence was observed, which became more pronounced at longer wavelengths.
- (l) Laser photolysis at 248 and 308 nm wavelengths coupled with gas-chromatographic analysis to determine the photodissociation quantum yield of acetone, ϕ . At 308 nm ϕ decreased with decreasing temperature ($T = 323\text{--}233$ K) and also decreased with increasing pressure ($p = 13\text{--}998$ mbar synthetic air). Water vapour has no effect on ϕ in disagreement with the conclusion of Aloisio and Francisco (2000).
- (m) The formation of CH_3 in the 248 or 266 nm PLP of acetone was examined using and its detection by transient absorption spectroscopy at 216.4 nm. Measurements were conducted at pressures between ~ 5 and mbar N_2 and temperature of 298 ± 3 K. $\phi(\text{CH}_3)$ was determined in back-to-back experiments relative to CH_3I photolysis at the same wavelength. For acetone at 248 nm, $\phi(\text{CH}_3)$ was greater than unity at low pressures ($=1.42 \pm 0.15$, extrapolated to zero pressure) confirming that a substantial fraction of the CH_3CO co-product can dissociate to $\text{CH}_3 + \text{CO}$ under these conditions. At $p \sim 1$ bar $\phi(\text{CH}_3)$ approached unity, indicative of almost complete collisional relaxation of the CH_3CO radical. At 266 nm, where the yields of CH_3 (and CH_3CO) were close to unity and independent of pressure, strongly suggesting that nascent CH_3CO is insufficiently activated to decompose.
- (n) Measurements of $\phi(\text{CH}_3\text{CO})$ following the 248 nm PLP of acetone at 248 nm and at 296 K, relative to CH_3CO reference systems. CH_3CO was detected using cavity ring-down spectroscopy at wavelengths between 490 and 660 nm. Measurements were performed between 80 and 892 mbar (He, N_2 bath gases) and the cited CH_3CO quantum yields are at the low-pressure limit, determined from a Stern-Volmer analysis of the observed increase in quantum yield with pressure, i.e.: $\phi(\text{CH}_3\text{CO}) = \phi^0(\text{CH}_3\text{CO}) + (\phi^\infty(\text{CH}_3\text{CO}) - \phi^0(\text{CH}_3\text{CO}) \times (k_q[\text{M}]/(k_q[\text{M}] + k_d)))$, where k_q and k_d are the quenching and decomposition rate coefficients for CH_3CO^* formed at 248 nm; for N_2 $k_q[\text{M}]/(k_d) (\times 10^{-19} \text{ cm}^3 \text{ molecule}^{-1}) = 0.8 \pm 0.2$. The quoted uncertainties are 2σ (95% confidence level) and include estimated systematic errors.
- (o) The overall quantum yield of photolysis of acetone ($\text{CH}_3\text{C}(\text{O})\text{CH}_3$) at 248 and 266 nm was measured using the pulsed laser photolysis technique. The organic photo-fragment radicals CH_3 and CH_3CO were detected indirectly as Br atoms using time-resolved resonance fluorescence following their reaction with Br_2 . Quantum yields for acetone photolysis were derived relative to yields of COCl_2 (at 248 nm) or Cl_2 (at 266 nm) in back-to-back experiments in which Cl atoms were scavenged by Br_2 to form Br. At 248 nm experiments were carried out at pressures between 80 and 1010.8 mbar of N_2 and temperatures 224, 234 and 298 K. The overall quantum yield was 0.98 ± 0.10 at 248 nm and, within experimental uncertainty, was independent of pressure and temperature in the ranges covered. At 266 nm and 298 K, the overall quantum yield was also close to unity, but with a weak dependence on bath gas pressure. These results at 266 nm confirm the previous 266 nm data (Khamaganov *et al.*, 2007) obtained at 298 K using a different experimental approach, in which the yield of CH_3 was measured directly.

- (p) The same method as used in (o) was used to determine the overall quantum yield of acetone photolysis at 300 and 308 nm, at several pressures (80 to 984 mbar) and at either 298 or 228 K. Chemical actinometry used photolysis of Cl₂ in back-to-back experiments at the same wavelength and under identical experimental conditions. The pressure and temperature dependent quantum yields obtained with this method are in good agreement with previous literature values and are reproduced using the parameterisation developed by Blitz et al. (2006). At these longer wavelengths Br formation kinetics deviated from that expected from reactions of CH₃ and CH₃CO alone and Br atoms were still observed at high yield even when the quantum yield of formation of CH₃ and CH₃CO was low. This is explained by the reactive quenching of thermalized triplet acetone (T₁) by the Br₂ added as radical scavenger. High yields of T₁ (>80%) at the highest pressure in this study indicate that any dissociation from the first excited singlet state (S₁) occurs in competition with intersystem crossing, with only a small degree of quenching to the (S₀) ground state.

Preferred Values

Temperature dependent cross sections (215-349 nm)

λ (nm)	$10^{20} \sigma$ (cm ²)	$10^3 A$ (K ⁻¹)	$10^5 B$ (K ⁻²)	$10^8 C$ (K ⁻³)	λ (nm)	$10^{20} \sigma$ (cm ²)	$10^3 A$ (K ⁻¹)	$10^5 B$ (K ⁻²)	$10^8 C$ (K ⁻³)
215	0.167	-10.46	8.346	-16.43	283	4.71	1.137	-1.350	3.272
216	0.180	-9.192	7.357	-14.51	284	4.62	0.8530	-1.158	2.943
217	0.196	-6.233	5.039	-10.01	285	4.54	0.6518	-1.023	2.714
218	0.212	-3.190	2.651	-5.359	286	4.44	0.4907	-0.9154	2.531
219	0.228	-1.002	0.9314	-2.003	287	4.36	0.3190	-0.7992	2.332
220	0.246	0.4104	-0.1807	0.1679	288	4.28	0.1109	-0.6586	2.092
221	0.270	1.567	-1.090	1.936	289	4.15	-0.1230	-0.5036	1.833
222	0.294	2.962	-2.183	4.058	290	4.06	-0.3698	-0.3426	1.568
223	0.318	4.839	-3.651	6.909	291	3.95	-0.6430	-0.1615	1.265
224	0.346	6.940	-5.293	10.09	292	3.82	-0.9625	0.05796	0.8847
225	0.380	8.598	-6.588	12.60	293	3.71	-1.316	0.306	0.4472
226	0.419	9.380	-7.200	13.79	294	3.57	-1.650	0.535	0.0477
227	0.456	9.551	-7.336	14.06	295	3.42	-1.905	0.699	-0.2168
228	0.492	9.705	-7.462	14.31	296	3.26	-2.084	0.796	-0.3430
229	0.535	10.08	-7.761	14.89	297	3.11	-2.234	0.867	-0.4086
230	0.584	10.41	-8.023	15.41	298	2.98	-2.391	0.942	-0.4824
231	0.637	10.39	-8.002	15.36	299	2.82	-2.590	1.055	-0.6387
232	0.693	10.01	-7.707	14.79	300	2.67	-2.915	1.277	-1.020
233	0.750	9.534	-7.332	14.06	301	2.58	-3.421	1.649	-1.709
234	0.815	9.138	-7.022	13.46	302	2.45	-4.008	2.091	-2.543
235	0.885	8.851	-6.799	13.02	303	2.30	-4.508	2.465	-3.248
236	0.956	8.638	-6.634	12.70	304	2.18	-4.858	2.715	-3.699
237	1.03	8.471	-6.504	12.45	305	2.05	-5.120	2.880	-3.959
238	1.11	8.318	-6.385	12.22	306	1.89	-5.433	3.062	-4.219
239	1.21	8.125	-6.235	11.93	307	1.75	-6.010	3.429	-4.805
240	1.30	7.861	-6.031	11.53	308	1.61	-6.986	4.096	-5.954
241	1.40	7.554	-5.793	11.07	309	1.49	-8.135	4.899	-7.370
242	1.50	7.268	-5.571	10.64	310	1.36	-8.897	5.415	-8.255
243	1.60	7.035	-5.390	10.29	311	1.24	-8.923	5.378	-8.097
244	1.72	6.838	-5.237	9.994	312	1.14	-8.494	5.001	-7.305
245	1.83	6.649	-5.093	9.718	313	1.06	-8.228	4.754	-6.772
246	1.95	6.472	-4.960	9.464	314	0.944	-8.445	4.881	-6.959
247	2.07	6.326	-4.850	9.256	315	0.837	-8.966	5.240	-7.592
248	2.20	6.210	-4.763	9.091	316	0.760	-9.409	5.528	-8.076
249	2.33	6.099	-4.680	8.936	317	0.684	-9.584	5.588	-8.085

250	2.47	5.972	-4.587	8.763	318	0.598	-9.736	5.596	-7.946
251	2.60	5.832	-4.486	8.576	319	0.523	-10.39	5.958	-8.433
252	2.74	5.697	-4.389	8.399	320	0.455	-11.80	6.869	-9.933
253	2.87	5.581	-4.306	8.249	321	0.411	-13.48	7.962	-11.75
254	3.01	5.483	-4.235	8.120	322	0.348	-14.59	8.600	-12.67
255	3.15	5.385	-4.164	7.989	323	0.294	-14.98	8.670	-12.47
256	3.30	5.261	-4.075	7.825	324	0.248	-15.39	8.743	-12.27
257	3.44	5.101	-3.961	7.620	325	0.210	-16.28	9.187	-12.77
258	3.57	4.932	-3.843	7.410	326	0.174	-17.09	9.588	-13.21
259	3.69	4.802	-3.756	7.262	327	0.141	-17.21	9.471	-12.68
260	3.81	4.746	-3.723	7.215	328	0.113	-16.92	9.048	-11.58
261	3.94	4.744	-3.730	7.239	329	0.0913	-16.66	8.672	-10.62
262	4.07	4.734	-3.729	7.246	330	0.0740	-15.94	7.979	-9.099
263	4.20	4.651	-3.674	7.155	331	0.0586	-13.93	6.340	-5.829
264	4.32	4.482	-3.559	6.956	332	0.0465	-10.93	3.969	-1.214
265	4.41	4.271	-3.416	6.712	333	0.0375	-8.186	1.847	2.840
266	4.49	4.087	-3.296	6.513	334	0.0311	-6.530	0.6289	5.067
267	4.56	3.983	-3.234	6.420	335	0.0248	-5.692	0.1022	5.880
268	4.64	3.969	-3.235	6.440	336	0.0199	-4.656	-0.5382	6.860
269	4.72	4.009	-3.273	6.524	337	0.0162	-2.090	-2.355	10.09
270	4.79	4.025	-3.294	6.577	338	0.0135	3.113	-6.237	17.33
271	4.87	3.935	-3.240	6.494	339	0.0113	11.01	-12.26	28.77
272	4.91	3.704	-3.085	6.231	340	00912	20.02	-19.22	42.15
273	4.94	3.378	-2.861	5.845	341	00729	27.20	-24.83	53.03
274	4.94	3.061	-2.645	5.473	342	00583	29.63	-26.80	56.96
275	4.94	2.854	-2.508	5.243	343	00494	25.97	-24.04	51.78
276	4.93	2.790	-2.474	5.201	344	00365	16.35	-16.63	37.55
277	4.92	2.816	-2.505	5.276	345	0.00301	3.774	-6.858	18.72
278	4.94	2.820	-2.518	5.316	346	0.00235	-2.414	-1.987	9.304
279	4.92	2.692	-2.433	5.175	347	0.00158	7.880	-9.888	24.53
280	4.91	2.389	-2.222	4.803	348	0.00111	29.52	-26.61	56.78
281	4.86	1.963	-1.922	4.272	349	0.00107	41.03	-35.51	73.95
282	4.79	1.517	-1.612	3.726					

$$\sigma(\lambda, T) = \sigma(\lambda, 298 \text{ K})[1 + A(\lambda)T + B_2(\lambda)T^2 + C(\lambda)T^3].$$

Quantum Yields

In atmospheric photolysis region:

$$\Phi_{\text{TOTAL}}(\lambda, [M], T) = \phi_{\text{CH}_3\text{CO}}(\lambda, [M], T) + \phi_{\text{CO}}(\lambda, T)$$

For $\lambda = 279\text{-}327.5$ nm

$$\phi_{\text{CO}}(\lambda, T) = 1 / (1 + A_0)$$

$$\text{where } A_0 = [a_0 / (1 - a_0)] \exp[b_0 \{\lambda - 248\}]$$

$$a_0 = (0.350 \pm 0.003) (T/295)^{(-1.28 \pm 0.03)}$$

$$b_0 = (0.068 \pm 0.002) (T/295)^{(-2.65 \pm 0.20)}$$

For $\lambda = 279\text{-}302$ nm

$$\phi_{\text{CH}_3\text{CO}}(\lambda, [M], T) = \{1 - \phi_{\text{CO}}(\lambda, T)\} / \{1 + A_1[M]\}$$

$$\text{where } A_1 = a_1 \exp[-b_1 \{(10^7/\lambda) - 33113\}]$$

$$a_1 = (1.600 \pm 0.032) \times 10^{-19} (T/295)^{(-2.38 \pm 0.08)}$$

$$b_1 = (0.55 \pm 0.02) \times 10^{-3} (T/295)^{(-3.19 \pm 0.13)}$$

For $\lambda = 302\text{-}327.5$ nm,

$$\phi_{\text{CH}_3\text{CO}}(\lambda, [M], T) = \{(1 + A_4[M] + A_3) / [(1 + A_2[M] + A_3)(1 + A_4[M])]\} \{1 - \phi_{\text{CO}}(\lambda, T)\}$$

$$\text{where } A_2 = a_2 \exp[-b_2 \{(10^7/\lambda) - 30488\}]$$

$$a_2 = (1.62 \pm 0.06) \times 10^{-17} (T/295)^{(-10.03 \pm 0.20)}$$

$$b_2 = (1.79 \pm 0.02) \times 10^{-3} (T/295)^{(-1.364 \pm 0.036)}$$

$$A_3 = a_3 \exp[-b_3 \{(10^7/\lambda) - c_3\}^2]$$

$$a_3 = (26.29 \pm 0.88) (T/295)^{(-6.59 \pm 0.23)}$$

$$b_3 = (5.72 \pm 0.20) \times 10^{-7} (T/295)^{(-2.93 \pm 0.09)}$$

$$c_3 = (30006 \pm 41) (T/295)^{(-0.064 \pm 0.004)}$$

$$A_4 = a_4 \exp[-b_4 \{(10^7/\lambda) - 30488\}]$$

$$a_4 = (1.67 \pm 0.14) \times 10^{-15} (T/295)^{(-7.25 \pm 0.54)}$$

$$b_4 = (2.08 \pm 0.02) \times 10^{-3} (T/295)^{(-1.16 \pm 0.15)}$$

In all cases quoted errors are 1σ , $[M]$ is in molecule cm^{-3} , λ in nm and T in K

In mid UV region:

at $\lambda = 248$ nm: $\phi_{\text{TOTAL}} = 1.0 \pm 0.05$ (independent of pressure and temperature)

at $\lambda = 248$ nm: $\phi_{\text{CH}_3\text{CO}}^0 = 0.55 \pm 0.05$ (independent of temperature)

$$\phi_{\text{CO}}^0 = 0.45 \pm 0.05$$

$$\phi_{\text{CH}_3}^0 = 1 + \phi_{\text{CO}}^0$$

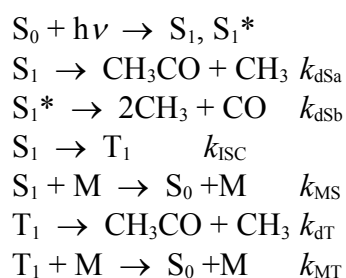
at $\lambda = 266$ nm: $\phi_{\text{TOTAL}} = 1.0 \pm 0.2$ (independent of pressure and temperature)

Comments on Preferred Values

The preferred absorption cross-sections are based on the measurements of Gierczak *et al.* (1998). They agree well with the room temperature measurements of Martinez *et al.* (1992) and Yujing and A.Mellouki (2000). Over the wavelength region 260 nm to 320 nm these cross-sections are within 5% of

earlier recommendations based on the data of Calvert and Pitts (1966) and Meyrahn *et al.* (1986). The cross-sections reported by Hynes *et al.* (1992) at room temperature contain large error limits at 320 nm and 340 nm but are in reasonable agreement with those recommended here. The recommended temperature dependent cross sections for 1 nm intervals over the range 215 – 349 nm, are based on the expression derived by Burkholder (as cited in the NASA Evaluation No 15, 2005), obtained by using a cubic fit to the data of Gierczak *et al.* (1998).

The absorption spectrum of acetone between ~210 and 340 nm corresponds to an $n\pi^*$ transition from the ground (S_0) to the first excited state (S_1). The mechanism of acetone photolysis is now well established and is supported by a large number of detailed photochemical and photodynamical studies over the past 40 years. Depending on excitation wavelength, the dissociation of acetone can occur directly via S_1 , or via a low-lying triplet state (T_1) formed by intersystem crossing. In either case, fission of the C–C bond occurs to form acetyl (CH_3CO) and methyl (CH_3) radicals. The quantum yield of CH_3 at 248 nm is > 1 , and CO is produced as a primary product. This is attributed to dissociation of energy-rich CH_3CO^* . The quantum yield for fluorescence or phosphorescence respectively from excited S_1 or triplet state (T_1) acetone is small and consequently is not included in the mechanism. The overall scheme is represented by the following reactions:



Extensive studies of the quantum yield for photodissociation of acetone over the past decade have provided reliable wavelength and pressure dependencies of ϕ and ϕ_1 [Gierczak *et al.* (1998); Emrich and Warneck (2000); Blitz *et al.*, (2004, 2006); Somnitz *et al.*, (2005); Khamaganov *et al.*, (2007); Nadasdi *et al.*, (2007); Rajakumar *et al.* (2008); Khamaganov *et al.*, (2009); Khamaganov and Crowley, (2013);]. The quantum yields at wavelengths below 300 nm and their pressure and wavelength dependence measured using a large number of different techniques are essentially in agreement. Both $\phi_{\text{CH}_3\text{CO}}$ and ϕ_{CO} have pressure dependence, and ϕ_{tot} at 1 bar falls off with wavelength above 280 nm. There is little temperature dependence in this region. The zero pressure limit value of ϕ_{tot} is unity at 248 nm. At longer wavelengths (> 300 nm) the study of Blitz *et al.* (2004, 2006) gave values of $\phi_{\text{CH}_3\text{CO}}$ substantially smaller than reported earlier, with a decrease of ϕ with temperature, which becomes more evident with increasing wavelength. At longer wavelengths overall quantum yields are influenced strongly by pressure quenching, which exhibits linear Stern-Volmer behaviour at wavelengths below 308 nm, but non-linear Stern-Volmer plots were reported at $\lambda > 308$ nm (Blitz *et al.*, (2004, 2006). Their pressure and temperature dependence results at longer wavelength have been confirmed by the subsequent measurements of photodissociation quantum yields at 300 nm and 308 nm and at 228 and 298 K (Nadasdi *et al.*, (2007) and Khamaganov and Crowley (2013).

The agreement provides strong support and reduced uncertainty for the optimized parameterization of the quantum yields given by Blitz *et al.* (2004) for the wavelength range 279-327.5 nm, temperature range 218 to 295 K and pressure up to 1000 mbar, for calculation of atmospheric photolysis rates (see also Arnold *et al.* (2004). This parameterisation is recommended in this evaluation for calculation of the preferred values of the overall quantum yields ($\phi_{\text{CH}_3\text{COCH}_3}$) in the range 279-327 nm and 218-295 K. Figure 1 shows comparison of observations at 300 and 308 nm of Khamaganov and

Crowley, (2013), Nadasti et al., (2007), Gierzeck et al. (1998), and the parameterisation given by Blitz et al. (2004) on the basis of a fit to their own experimental data. The parameterisation well reproduces the pressure and temperature dependent quantum yields in this atmospherically important region.

The recent studies provide further constraints on the photodissociation mechanism. The work of Somnitz et al, (2005) indicated that at 248 nm CO derives only from dissociation of excited CH_3CO^* and not by a direct/concerted channel from the excited singlet state of acetone. Increasing pressure and wavelength causes ϕ_{CO} to decrease, and $\phi_{\text{CH}_3\text{CO}}$ to increase. The direct measurements by Khamaganov et al., (2007) and Rajakumar et al. (2008) of pressure quenching of ϕ_{CH_3} and $\phi_{\text{CH}_3\text{CO}}$ respectively at 248 nm supports this result; these results for zero pressure quantum yields of $\phi_{\text{CH}_3}^0 (= 1.42 \pm 0.15)$ and $\phi_{\text{CH}_3\text{CO}}^0 (= 0.539 \pm 0.09)$ are in very good agreement and provide the basis of our preferred values at this wavelength. At 266 nm, $\phi_{\text{CH}_3} = 0.93 \pm 0.1$ and is independent of pressure, showing that no dissociation of internally excited CH_3CO occurs at this wavelength. Further experimental measurements by Khamaganov et al., (2009) of the overall photo-dissociation quantum yield, ϕ_{total} , at 266 nm using the Br_2 scavenging method shows a weak pressure quenching of ϕ , consistent with the results of Gierzeck et al. (1998) but in conflict with inferences from ϕ_{CO} measurements of Gandini and Hackett, (1977) and Meyrahn et al. (1986), and with the low CH_3CO yields observed by Blitz et al (2006), which were not fitted by their parameterisation based on a global fit over an extended range of longer wavelengths. Studies at longer wavelengths (300 and 308 nm) using the Br_2 scavenging method (Khamaganov and Crowley, 2013) has shown that triplet acetone (T_1) is formed by ISC from the S_1 state, with high efficiency which increases with pressure, in line with the conclusions of a review by Haas (2004).

References

- Arnold, S. R., Chipperfield, M. P., Blitz, M. A., Heard, D. E. and M. J. Pilling, *Geophys. Res. Lett.* L07110, doi:10.1029/2003GL019099, 2004.
- Aloisio, S. and Francisco, J. S., *Chem. Phys. Lett.* 329, 179, 2000.
- Blitz, M. A., Heard, D. E., Pilling, M. J., Arnold S. R. and M. Chipperfield, *Geophys. Res. Lett.* L06111, doi:10.1029/2003GL018793, 2004.
- Blitz, M.A., Heard, D. E. Heard, and Pilling, M. J., *J. Phys. Chem. A*, 110, 6742, 2006
- Calvert, J. G., and Pitts, Jr., J. N., *Photochemistry*, Wiley, New York, 1966.
- Emrich, M. and Warneck, P., *J. Phys. Chem. A* 104, 9436, 2000.
- Gandini, A. and Hackett, P.A., *J. Am. Chem. Soc.*, 99, 6195, 1977
- Gierczak, T., Burkholder, J. B., Bauerle, S. and Ravishankara, A. R., *Chem. Phys.* 231, 229, 1998.
- Haas, Y., *Photochem. Photobiol. Sci.*, 3, 6 - 16, (2004)
- Hynes, A. J., Kenyon, E. A., Pounds, A. J., and Wine, P. H., *Spectrochim. Acta* 48A, 1235, 1992.
- Khamaganov, V., Karunanandan, R., Rodriguez, A. and Crowley, J. N., *Phys. Chem. Chem. Phys.*, 9, 4098, 2007.
- Khamaganov, V., Karunanandan, R., A. Horowitz, T. J. Dillon and Crowley, J. N., *Phys. Chem. Chem. Phys.*, 11, 6173, 2009.
- Khamaganov, V., and Crowley, J., *Phys. Chem. Chem. Phys.*, 15, 10500, 2013.
- Martinez, R. D., Buitrago, A. A., Howell, N. W., Hearn, C. H. and Joens, J. A., *Atmos. Environ.* 26A, 785, 1992.
- Meyrahn, H., Pauly, J., Schneider, W. and Warneck, P., *J. Atmos. Chem.* 4, 277, 1986.
- Nadasdi, R., Kovacs, G., Szilagyi, I., Demeter, A., Dobe, S., Berces, T., Marta, F., *Chemical Physics Letters* 440, 31, 2007.
- Rajakumar, B., Gierczak, T., Flad, J. E., Ravishankara, A.R., Burkholder J B., *J Photochem. and Photobiol. A: Chemistry* 199, 336, 2008
- Somnitz, H., Fida, M., Ufer, T. and Zellner, R., *Phys. Chem. Chem. Phys.*, 7, 3342, 2005.

Warneck, P., *Atm. Environ.* 35, 5773, 2001.

Yujing, M. and Mellouki, A., *J. Photochem and Photobiol. A: Chemistry* 134, 31, 2000.

Figure 1: Pressure dependence of ϕ_{total} for photolysis of acetone at 308 nm and 298 and 228 K. Data from Khamaganov and Crowley, (2013), Nadasdi et al., (2007), Gierczak, et al (1998) and parameterisation given by Blitz et al. (2004), which is adopted in this IUPAC recommendation.

